

Monitoring Fishmeal & Fish Oil production near Gunjur (The Gambia) with 3m PlanetScope Imagery: An Exploration

Abstract

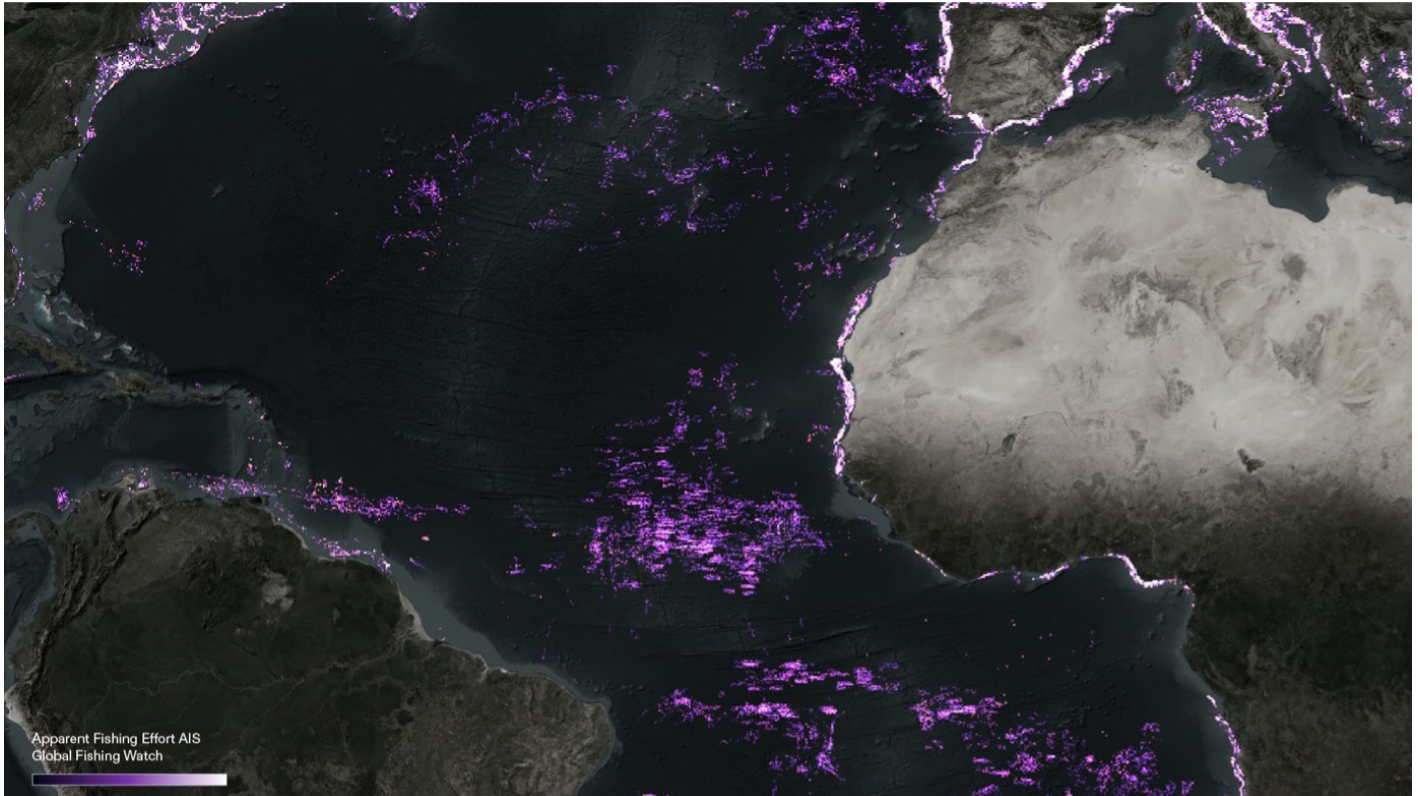
Artisanal fishers in Senegal and The Gambia are increasingly caught between offshore industrial fishing and a fast-growing shore-based fish meal/fish oil (FMFO) industry. While the impact of the former has been the subject of numerous studies that have tried to detect and quantify the scale of fish stock depletion it is responsible for, the latter has so far received far less attention. Even if the disastrous effects of FMFO production in The Gambia – and more generally along the West African coast – have been amply denounced by local populations as well as international organizations and journalists. In the absence of any official data monitoring FMFO production in The Gambia this study sets out to develop a model for detecting and documenting the activities and locations of artisanal fishing fleets, upon which the FMFO factories depend.

This preliminary study focuses on in the Gambian coastal village of Gunjur, where the Golden Lead FMFO factory opened in 2016. The study employs remote sensing techniques to detect the presence of artisanal fishing vessels gathering to land their catch in the Bay of Gunjur during the 6 months of FMFO factories activity, between November and June. This framework allows for the study of changes in the activities and numbers of artisanal fishing brought about by the factory's operations. Whilst providing insights into practices of temporary migration between Senegal and The Gambia driven by FMFO production.

We present an open, reproducible workflow that applies simple spectral indices to fourteen PlanetScope scenes (2018–2024, 3 m spatial resolution) to detect small wooden and fiberglass boats operating in Gunjur Bay. A scene-specific Normalised Difference Water Index (NDWI) threshold, morphological cleaning and 4 connected component analysis isolate vessel footprints. Early counts illustrate the potential for community-led oversight while underscoring the caution required when drawing conclusions from single and isolated snapshots. This methodology lays the ground work for further in-depth studies with increased access to satellite imagery, providing deeper insights changes in artisanal fishing practices following the emergence of West Africa as a crucial FMFO global exporter. Conversely, it must be noted that the number of boats provides only an indirect—and imperfect—proxy for estimating the volume of fish stock consumed by factories, as vessel presence alone does not reflect catch size, fishing effort, or ultimate usage.

Introduction

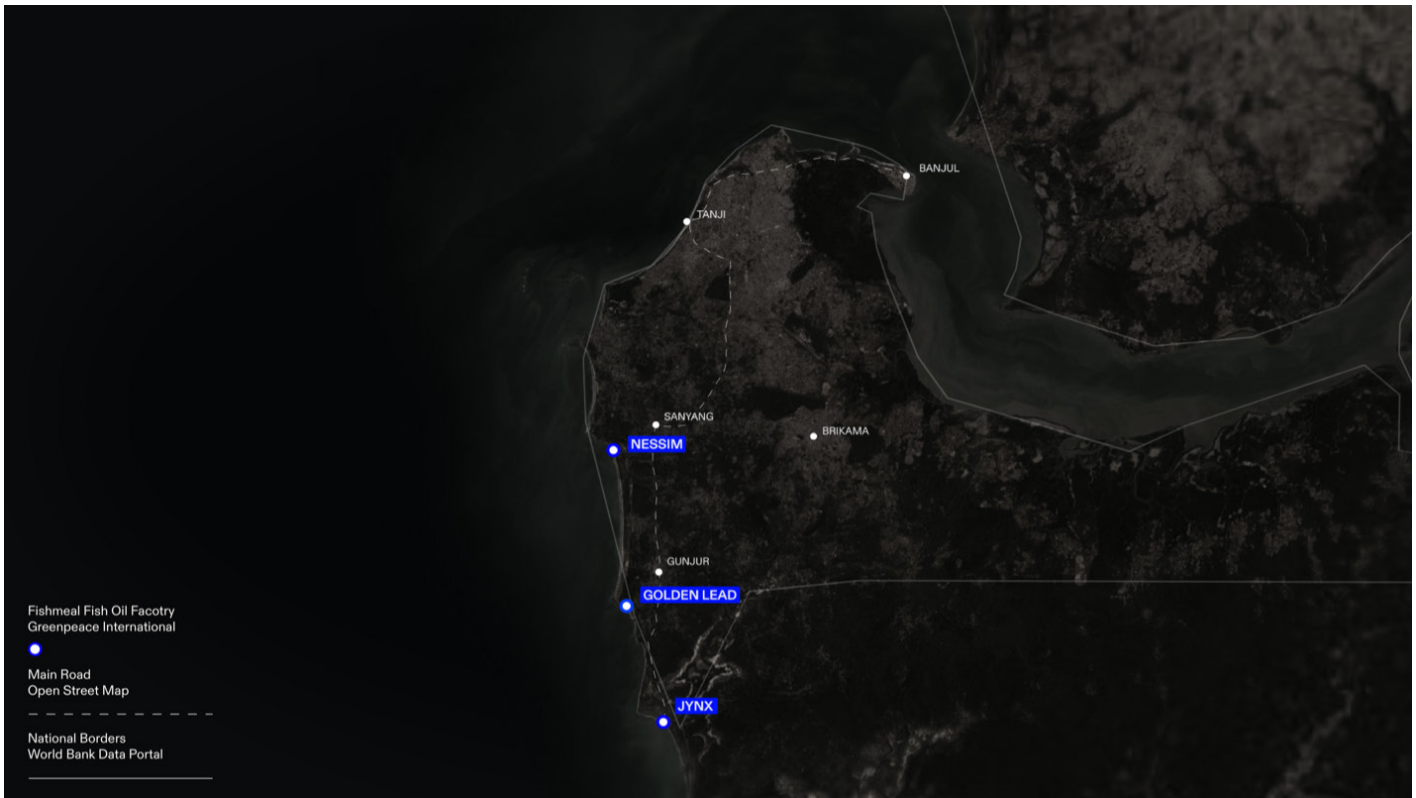
In recent years, the waters off West Africa have become a crucial component in the increasingly globalized fishing industry, supplying farms and consumers throughout Asia, the Americas and Europe with the region's most vital staple: fish. A process of acute extraction, orchestrated through an increasing number of foreign fishing fleets, obtaining access to West Africa's abundant marine ecology through political agreements as well as illegal fishing practices.



Since 2005, over forty factories dedicated to the production of fishmeal and fish oil (FMFO) have been established along the coastline, processing locally consumed species of fish such as *Sardinella* and *Bonga* into flour, pellets, and oil primarily destined for global aquaculture and animal-farming markets. The Gambia, West Africa's smallest mainland state and one of its most fish-dependent, hosts three predominantly Chinese-owned FMFO plants established between 2015 and 2018. Collectively they purchase an estimated 80 % of all fish landed nationwide, concentrating both economic power and ecological pressure on a coastline less than 80 km long. The largest, Golden Lead at Gunjur, sits directly on the migration corridor of the *Sardinella* and *Bonga* fish, robbing Gambian communities of both their primary source of protein and a lifeworld built around fishing.

Map showing all apparent fishing effort in Jan 2023 as collected by Global Fishing Watch using AIS databases

Local resistance has grown in parallel with production. In 2018 sustained protests forced the removal of an ocean-going wastewater pipe at The Golden Lead factory that discharged untreated effluent into the bay – only for the pipe to be reinstalled four months later under a police escort. Three years on, violent clashes at the Nessim factory in Sanyang left one man dead and the plant in flames, because of heavy-handed police response. Activists describe an atmosphere of secrecy surrounding factory operations, with freedom of information requests routinely ignored, official monitoring data withheld and cases of corruption of local officials in charge of FMFO production oversight documented by investigative news outlets.



To better understand how artisanal fishing fleets have responded to the factories' operations, and indeed how these operations have affected the activities of artisanal fishing fleets, several key dynamics must be outlined. Production typically occurs over a six-month period, between November and June. Importantly, there are no designated landing bays in the vicinity of the factories—and, in fact, only one exists in the entire country—making it logistically infeasible for larger scale industrial fishing fleets to supply them. Hence, traditional fishing vessels, or pirogues, serve as the main providers. However, boats operated by local Gambian fisherfolk are typically too small to guarantee the volume and consistency required by the fish-hungry factories. As a result, larger boats from neighboring fishing communities are often 'hired' or 'contracted' to supply fish. These vessels go out daily and return with their catch, which is then brought into the factory by casual laborers using baskets.

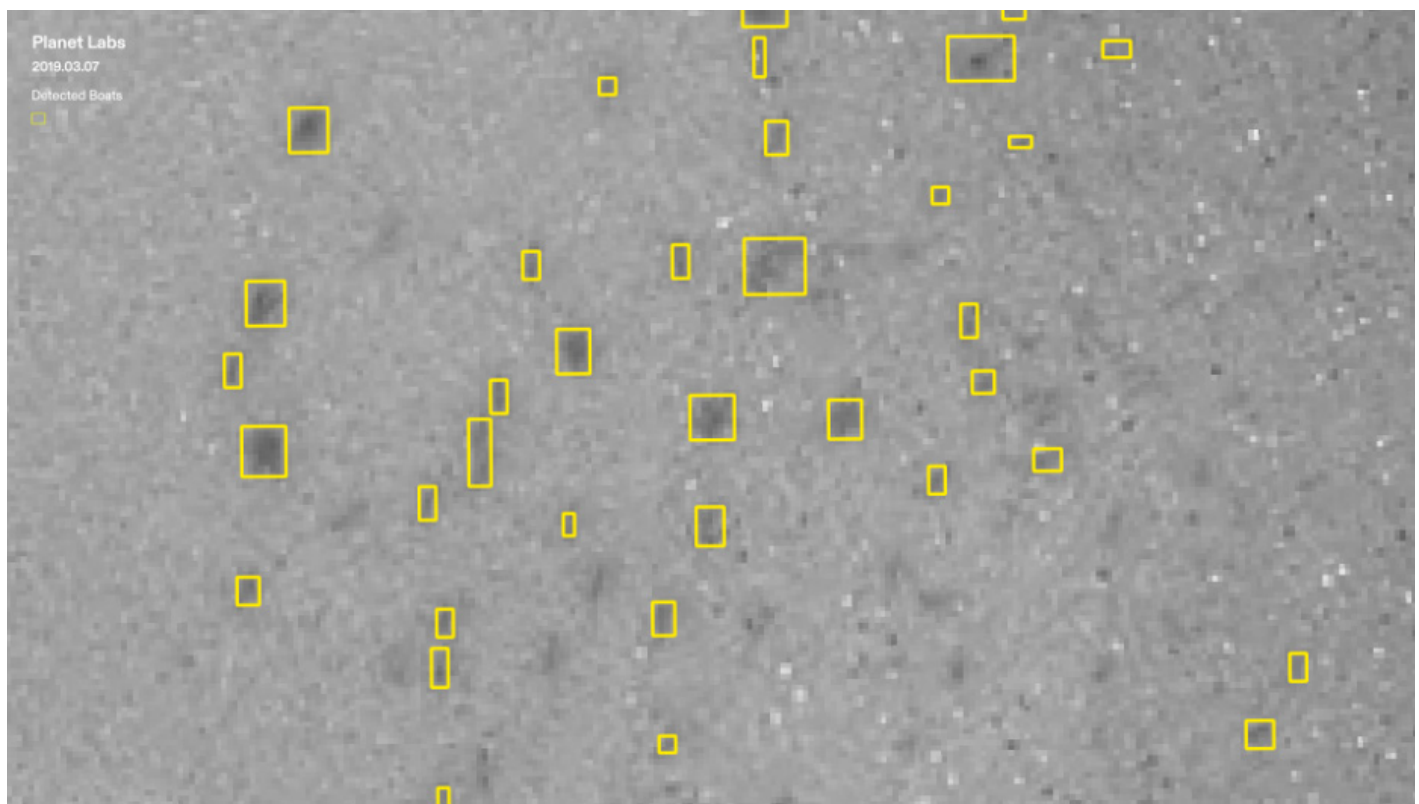
Map showing the locations of FMFO factories at key fishing villages along The Gambian Coast



Boats landing their catch at the FMFO factory at Kartong Beach, in Southern Gambia

Fishermen are paid per basket, which becomes the sole metric for quantifying the amount of fish delivered to the factory. However, these basket-based records are not disclosed by the factories, rendering the actual volume of intake opaque. Some local monitoring efforts have attempted to collect such data independently. In this context, reliable statistics on artisanal landings and factory intake remain elusive. Whilst most pirogues, the traditional fishing vessels which in The Gambia are responsible for the provision of fish to the FMFO factories, lack Automatic Identification System (AIS) beacons which prevents monitoring of the situation.

Given this absence of formal data, this study pilots the location and quantification of vessels at Gunjur Bay as an indirect—and admittedly imperfect—proxy for estimating both fishing stress and temporary migration patterns in artisanal fishing fleets. This approach assumes, based on extensive fieldwork, that no other comparably significant driver of fishing effort has emerged during this period. This understanding is grounded in fieldwork conducted by team members Lorenzo Pezzani, Jack Isles and Dr Alagie Jinkang over 18 months, including over 30 formal interviews and multiple periods of direct observation at landing sites and factory perimeters.



Planet Labs' daily, 3m imagery offers a timestamped, independent record of what is—literally—on the water. While each snapshot is imperfect, a sequence of snapshots can reveal patterns. Crucially, Planet data are commercially accessible at research rates and viewable through free web interfaces, enabling civil society groups to inquire on factory activities without expensive hardware.

Planet labs' daily 3m image with boats highlighted in yellow bounding boxes

This study has 3 main goals:

- 1 Craft and document a minimalist detection algorithm that runs on a laptop and requires no machine learning training data.
- 2 Apply the workflow to fourteen cloud-free scenes covering seven years to gauge its practical utility.
- 3 Reflect on what single-moment vessel counts can —and cannot— say about fishing efforts and coastal livelihoods.

Data and Methods

The study area is defined as Gunjur Bay (13°25' N, 16°46' W), which includes the Golden Lead factory and the landing site used to deliver fish to the factory (see figure below). To delineate its spatial extent, high-resolution PlanetLabs imagery was employed.



Image of study area defined over Gunjur bay

Satellite data

Fourteen orthorectified PlanetScope Surface Reflectance (PSScene4-8Band) tiles with less than 5 % cloud cover were selected. Acquisition times ranged from 09:59 to 12:16 UTC to ensure comparable solar illumination and fishing-activity conditions. For each month of March and April between 2018 and 2024, we reviewed several candidate images and retained only one per month based on the following quantitative criteria: minimal sun glint, minimal surface-wave interference, and maximal vessel visibility. By choosing, for each month, the single image that exhibits the highest number of boats (among all low-glare, low-wave tiles), we ensure a consistent representation of peak fishing activity across the study period, even in the absence of daily acquisitions.

Processing workflow – plain language overview

First, we create a true-color image by stacking the red, green, and blue bands, resulting in a composite that is immediately recognizable and inspectable by any analyst. From this composite, we calculate the Normalized Difference Water Index (NDWI), which accentuates open water (bright) and suppresses other features such as land, boats, and glare (dark). Because atmospheric conditions—such as cloud cover, suspended sediments, and sun glint—vary from one acquisition to the next, the optimal NDWI threshold cannot be predetermined. We employed a systematic, image-by-image approach: for each scene, we test a sequence of candidate thresholds (typically ranging

from 0.1 to 0.4) and select the one that most effectively separates water from boats and other bright artifacts. Under calm, clear-water conditions, thresholds around 0.10–0.15 generally suffice; in contrast, when turbidity is high or sun glint is pronounced (for example, during hazier afternoons), a higher threshold—up to 0.25–0.30—is required to prevent misclassifying glint-contaminated or sediment-loaded water as vessels. All pixels with NDWI values above the chosen threshold are labeled as “water,” while pixels below the threshold are retained as potential vessel candidates or non-water noise.

Once the initial binary water mask is generated, we apply a 3×3 mode filter to eliminate “salt-and-pepper” noise—small clusters of pixels that might represent wave crests, foam, or fleeting glint rather than actual boats. Each pixel is replaced by the most frequently occurring value in its 3×3 neighborhood, thereby removing isolated misclassifications without disturbing contiguous water areas or actual boats. After mode filtering, we quickly clean the mask by filling in small holes and removing narrow gaps. This produces a smooth, continuous water mask so that genuine boats are not broken up in later steps. It ensures that small imperfections do not fragment the shapes of legitimate vessels in later steps.

Next, we crop the cleaned water mask to the polygon outlining Gunjur Bay by rasterizing that polygon. This step eliminates from consideration surf-zone foam, breaking waves along the shoreline, and nearshore turbidity. The resulting mask contains only true water pixels within the bay’s legal boundary. To detect individual vessels, we invert this water mask which turns boats and other dark features into bright dots. We then run a connected-component analysis using 4-connectivity—meaning that pixels are grouped only if they share a full edge, not merely a corner—so that each cluster represents a contiguous object. Clusters whose pixel area falls between 6 and 300 are retained as potential boats: clusters smaller than 6 pixels are likely foam flecks or residual noise, while clusters larger than 300 pixels are more likely sandbars, dock shadows, or substantial glint artifacts. The remaining clusters become our final ship candidates.

Finally, we overlay red bounding rectangles around each detected cluster on both the true-color composite and the NDWI layer, producing annotated images that allow a human analyst to perform a rapid double check before any further analysis. In practice, this entire workflow—from band stacking through vessel annotation—executes in under 30 seconds per image on a standard laptop.

Technical workflow – reproducible details

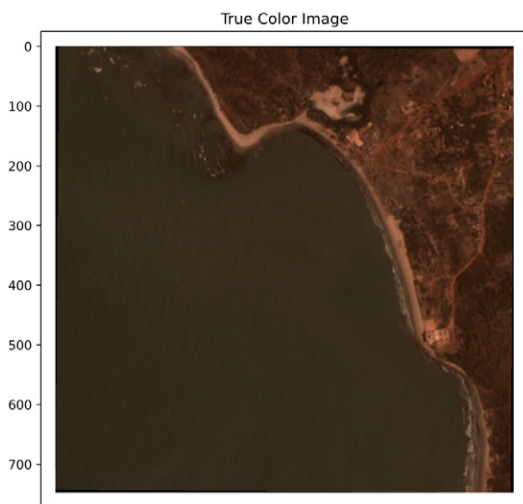
Below, we unpack each processing step in sufficient detail to ensure that the method and workflow are fully replicable. The complete Python script (including all preprocessing, NDWI calculation, mask generation, and vessel-detection routines) is provided in Annex. To run the workflow as described, you will need a Python 3 environment with the following packages installed:

- **numpy** (for array operations)
- **matplotlib** (for image plotting and annotation)
- **scipy** (specifically `scipy.stats` and `scipy.ndimage` for mode filtering, morphological operations, and connected-component labeling)
- **GDAL/OGR** (via the `osgeo` bindings, for reading the multispectral TIFF and rasterizing the bay polygon)
- **rasterio** (for writing out georeferenced GeoTIFFs)
- **geopandas** and **shapely** (for any vector-based manipulations, although most raster/vector interoperability is handled via GDAL)
- **mpl_toolkits.axes_grid1** (for fixed-position colorbars when plotting NDWI)

Before beginning, ensure that these libraries (and their dependencies) are correctly installed in your Python environment so that all code cells in the script execute without error

True color composite (RGB)

The surface-reflectance file arrives as multiple separate bands including at least one each for blue, green, red, and near-infrared. We combine the three visible bands—red, green, and blue—into a single three-layer array, then linearly rescale each layer to the 0–255 range so that the image looks like a familiar true-color photograph. In this composite, boat bodies appear as light-colored shapes against darker water. We save this result both as an 8-bit GeoTIFF (preserving georeferencing) and as a simple PNG for use in figures.

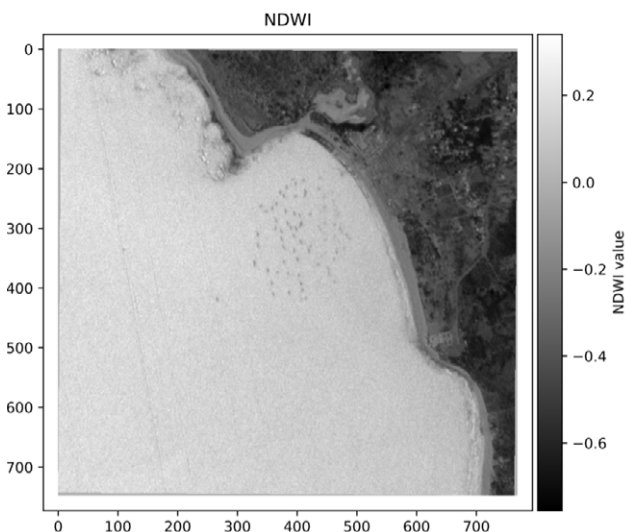


NDWI calculation

To isolate water surfaces from land, vessels, and other features, we compute the Normalized Difference Water Index (NDWI) as follows:

$$\text{NDWI} = (G - \text{NIR}) / (G + \text{NIR} + \epsilon)$$

where G and NIR denote the green and near-infrared-band reflectance values (each converted to floating-point) and ϵ is a small constant introduced to prevent division by zero over very dark pixels. The resulting NDWI raster has values spanning approximately -1 to +1 and is preserved in floating-point format for diagnostic and post-processing purposes.



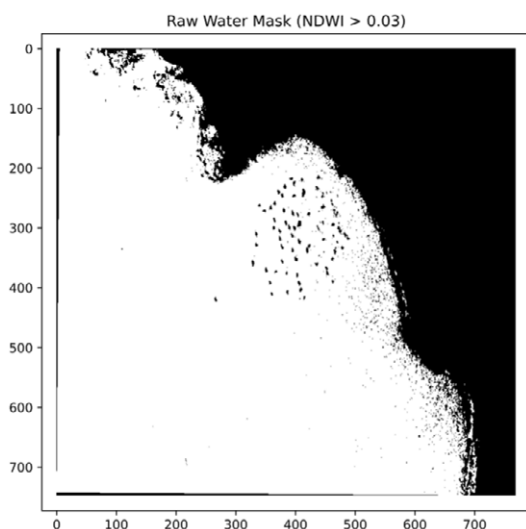
Physically, water bodies absorb strongly in the near-infrared wavelength region while reflecting moderately in the green portion of the spectrum. By taking the normalized difference, pixels corresponding to open water tend to yield high positive NDWI values (often > 0), whereas non-water features—vegetation, built-up areas, bare soil, and boats—typically produce NDWI values near zero or negative. In practice, NDWI is widely used in remote sensing to enhance water detection because it accentuates these spectral differences. However, it is also known to be sensitive to built-up or highly reflective urban surfaces, which can partially mimic the spectral signature of water if strong green reflectance coincides with moderate NIR reflectance. In our workflow, we leverage NDWI’s ability to emphasize water pixels while being mindful of potential false positives over bright non-water areas; subsequent thresholding and morphological filtering mitigate misclassifications.

The NDWI raster—computed on a per-pixel basis across the entire scene—is then stored as a georeferenced, single-band GeoTIFF. This floating-point NDWI layer serves as the foundation for all downstream binary water-masking and vessel-detection steps.

Scene specific threshold selection

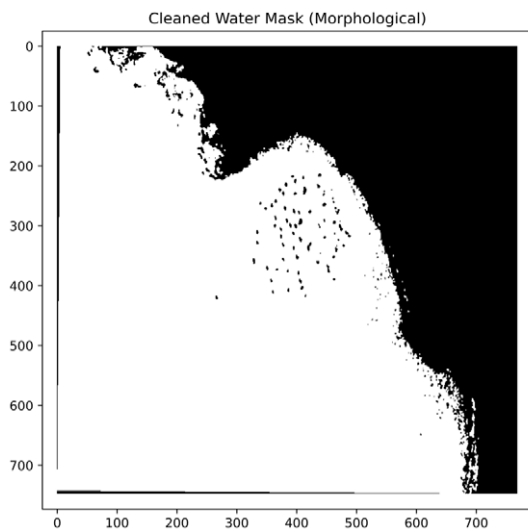
An NDWI threshold is applied directly to the floating-point NDWI raster to produce a binary water mask. Concretely, all pixels with an NDWI value greater than the threshold are set to “1” (water), while all other pixels are set to “0” (non-water or background). In practice, this means that, once an analyst has visually inspected the true-color and NDWI layers (for example, by overlaying a preliminary binary mask in a GIS), they assign a scene-specific threshold τ —typically between 0.10 and 0.30—such that open water remains uniformly flagged as “1” while boat and other non-water features are assigned “0.”

This thresholding step is pivotal for downstream vessel detection because it ensures that the water surface forms a contiguous, high-value region, while boats (whose structure absorb more in the NIR band and thus yield lower NDWI) appear as “holes” or “0” pixels embedded in that sea of ones. By isolating water pixels first, we can later invert the mask and perform connected-component labeling on these dark regions to extract candidate boat shapes. If the threshold is set too low, foamy surf or sun-glint-affected water may be misclassified as “0” (false positives), causing false detections; conversely, if the threshold is too high, small vessels may remain “1” (false negatives), resulting in missed detections. Thus, selecting an appropriate NDWI cutoff for each scene is crucial to maximizing both the precision and recall of boat identification.



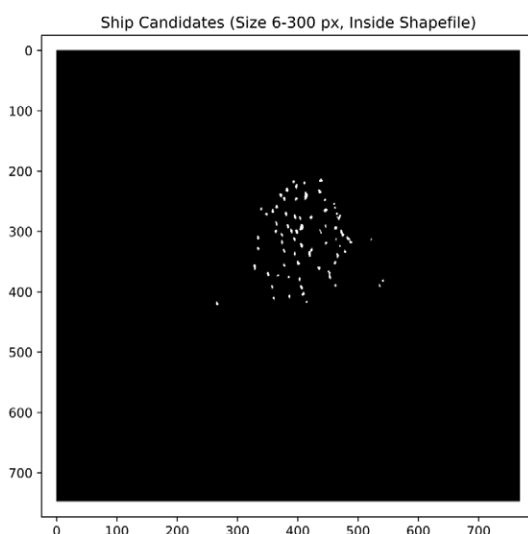
Noise suppression and morphological cleaning

The raw binary water mask often contains isolated “pepper” pixels (false non-water) and tiny holes that can fragment real vessels. A 3×3 mode filter replaces each pixel with the most common value in its neighborhood, removing single-pixel noise without blurring boat edges—since vessels span many pixels, their overall shape remains intact. Any remaining one-pixel indentations or thin non-water threads are healed by a single closing (dilate→erode) to fill small holes, followed by a single opening (erode→dilate) to remove narrow thin lines. Because real boats occupy at least six connected pixels, these morphological steps alter at most one-pixel-wide artifacts and do not eliminate legitimate vessels. The result is a smooth, gap-free water mask in which all genuine boats remain as contiguous clusters.



Spatial constraint (ROI masking)

Next, we restrict our analysis to water within the official boundaries of Gunjur Bay by rasterizing the bay polygon and applying it as a mask to the cleaned water layer. This step effectively removes breaking surf along the sandbar and spray over the reef of the study area, ensuring that only true water pixels inside the bay are retained for vessel detection.

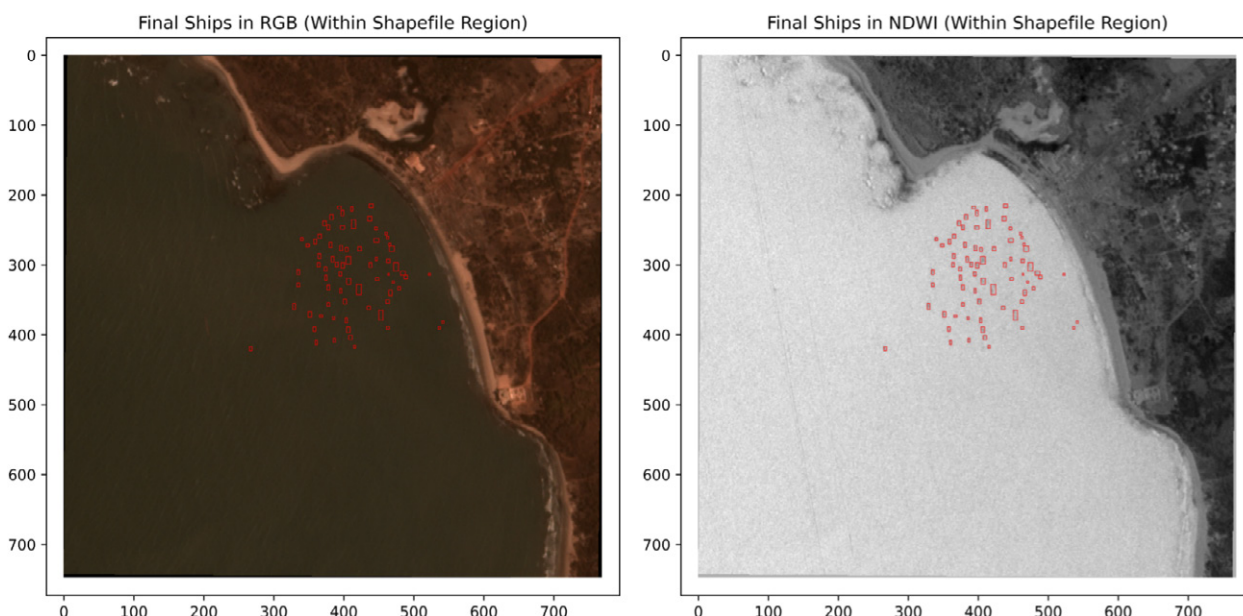


Connected component extraction and size filtering

After isolating only the water inside Gunjur Bay, we flip that water mask so that any boat structure—which appeared as gaps in the water—now become bright, isolated shapes. Each of these bright shapes is a candidate boat. We then group all adjacent bright pixels into individual “blobs,” treating any directly touching pixels as part of the same object. Blob detection here simply means finding every group of touching “white” pixels (boats) in a black-and-white image. We scan the image and assign a unique label to each contiguous cluster of white pixels, where “touching” means sharing an edge (up, down, left, right). After labeling, we count how many pixels belong to each cluster and keep only those whose size matches a realistic boat footprint (6–300 pixels). Each remaining cluster is then treated as one detected vessel. Any cluster smaller than a small canoe or larger than a large commercial boat is discarded as noise or a non-boat feature. For each remaining blob, we draw the smallest possible rectangle that entirely encloses it. Those rectangles are then exported as a GeoJSON file (retaining the original map projection), so that each detected vessel can be easily plotted, counted, or reviewed in any standard mapping software.

Output generation and visual QA

For human validation we draw 0.4 pt red rectangles around each candidate on both the NDWI greyscale image and the RGB composite using Matplotlib.



Results

3.1 Overview of scenes processed

Fourteen cloud free PlanetScope scenes spanning March 2018 to April 2024 passed the workflow (Table 2). Acquisition times range from late morning (09:59 UTC) to early afternoon (12:16 UTC), trying to remain consistent in the fishing moment of the day.

Table 2 — Scene catalogue and preliminary vessel counts.

Year	Scene ID	Date	Local time (UTC+0)	NDWI Threshold	Detected vessels
2018	20180309_110118_0f18_3B_AnalyticMS_SR_clip	2018-03-09	11:01	0.15	33
	20180423_110301_1038_3B_AnalyticMS_SR_clip	2018-04-23	11:03	0.15	42
2019	20190305_105859_0f2d_3B_AnalyticMS_SR_clip	2019-03-05	10:58	0.28	53
	20190427_121642_68_1069_3B_AnalyticMS_SR_clip	2019-04-27	12:16	0.01	57
2020	20200316_100229_1020_3B_AnalyticMS_SR_clip	2020-03-16	10:02	0.15	84
	20200405_095913_0f4d_3B_AnalyticMS_SR_clip	2020-04-05	9:59	0.03	71
2021	20210305_115529_67_1064_3B_AnalyticMS_SR_clip	2021-03-05	11:55	0.15	99
	20210425_104746_60_2420_3B_AnalyticMS_SR_8b_clip	2021-04-25	10:47	0.32	100
2022	20220301_104454_70_241f_3B_AnalyticMS_SR_8b_clip	2022-03-01	10:44	0.31	102
	20220406_111204_65_24a5_3B_AnalyticMS_SR_8b_clip	2022-04-06	11:12	0.25	92
2023	20230304_104035_03_241e_3B_AnalyticMS_SR_8b_clip	2023-03-04	10:40	0.42	99
	20230420_103534_16_2423_3B_AnalyticMS_SR_8b_clip	2023-04-20	10:35	0.42	106
2024	20240312_105129_92_24af_3B_AnalyticMS_SR_8b_clip	2024-03-12	10:51	0.42	127
	20240409_105524_74_24af_3B_AnalyticMS_SR_8b_clip	2024-04-09	10:55	0.26	139

Over the seven-year period from 2018 through 2024, the number of vessels detected in Gunjur Bay exhibits a pronounced upward trend, punctuated by year-to-year fluctuations that reflect both fishing effort and environmental factors influencing detectability. In 2018, the two March and April scenes produced vessel counts of 33 and 42, respectively, yielding an average of 37.5 boat. By 2019, this average rose to 55.0 boats—an increase of approximately 47% over the previous year. The momentum continued into 2020, where counts averaged 77.5, representing a further 41 % rise from 2019. The peak of this early upward trajectory occurred in 2021, when imagery recorded a mean of 100. These successive annual gains suggest a genuine intensification of fishing activity in addition to consistently favorable imaging and detection conditions that made boats easily visible with this method.



Some slight declines or constant ship counts can be observed. These declines could arise from several factors: a temporary reduction in fleet presence, perhaps due to seasonal shifts; or rougher surf and higher turbidity that impeded detection.

Finally, 2024 exhibits the most dramatic jump in our series: March 2024 recorded 127 vessels. It may also reflect algorithmic improvements or especially low turbidity on that date ($\tau = 0.42$ in March 2024). In April 2024, the threshold was lowered to 0.26, suggesting that analysts judged conditions (e.g., slight turbidity or minor glint) required a different cutoff.

Algorithm performance

Every remote-sensing and automated detection workflow carries some degree of uncertainty, because true ground-truth validation (for example, very-high-resolution imagery acquired at the exact same moment) is not available. In our case, complete ground truth is impossible: there are no synchronous, centimeter-scale aerial photos or exhaustive on-the-water boat counts for every PlanetScope overpass. Instead, we assessed performance by manually inspecting a selection of scenes—particularly those with clear water and well-separated boats—comparing the algorithm’s vessel detections against what was plainly visible in the true-color composites and NDWI image. In these “best-case” images, where boats are neither obscured by surf nor merged into dense clusters, manual counting confirmed that the automated workflow missed fewer than 10 % of vessels.

That residual error stems from two main factors. First, small boats—especially those under six meters—sometimes occupy too few pixels and get deleted by the successive filters. Second, when multiple boats raft tightly together, the algorithm occasionally merges them into a single blob and undercounts by one vessel. In scenes free of extreme turbidity, surf, or heavy clustering, these two effects combined contributed to an overall miss-rate of less than 10 %. While that figure reflects only a subset of ideal conditions, it provides a realistic ceiling on our method’s error under favorable imaging and thresholding scenarios. Consequently, users should interpret vessel counts as accurate to within approximately ± 10 % in the clearest, most interpretable scenes, with larger uncertainty—potentially up to 15 %–20 %—when water clarity is poor or boats are tightly grouped.

Discussion

Satellite snapshots—even when sparse—offers good data insights surrounding Gunjur’s fishing economy. Our method demonstrates that a single multispectral index, adjusted per scene, suffices to map medium-sized pirogues without relying on expensive, proprietary imagery or bespoke machine-learning training data. The algorithm is straightforward to understand, and the hands-on thresholding approach makes it accessible to non-specialists. By distributing open-source code alongside side-by-side visual outputs, we foster transparency and enable community observers, journalists, and local stakeholders to audit or replicate the workflow.

Nevertheless, the very simplicity that renders this method portable also imposes certain limitations. A satellite image is merely a snapshot in time: a calm anchorage at late afternoon may simply indicate a random and punctual decrease in activity rather than a true absence of boats.

At 3 m resolution, six-meter boats hover on the edge of detectability, and vessels navigating side by side frequently merge into a single blob, complicating precise counts. Environmental noise—sun glint, sediment plumes, or afternoon cumulus—can occasionally pass through threshold tuning, leading to false positives or missed detections. Moreover, scene-specific threshold selection, despite its pragmatic advantages, introduces a degree of subjectivity that complicates strict time-series comparisons across images. Quantifying precision remains challenging in the absence of perfectly synchronous ground truth; however, manual inspections on clearer scenes suggest error rates of less than 10 %, which provides sufficient confidence for many practical applications.

Local monitoring of the amount of fish brought into the factories—particularly through the counting of baskets by appointed independent monitors from local associations—could provide a valuable index of fish landings. This would allow for a more precise assessment of the validity of the satellite-based method, offering ground-level verification against which vessel counts and estimations of fishing stress could be calibrated.

Even so, imperfect vessel counts yield real-world value. Community groups can combine satellite-derived counts with others local issues which relate to the factories and their. Meanwhile, by teaching local activists and stakeholders to run the detector themselves, the workflow demystifies both satellite data and fishing supply chains.

Our findings already corroborate ground-truth testimonies from fishers and local observers: small-scale fishing effort in Gunjur has increased over the past several years – even considering the aforementioned limitations. Scaling from

fourteen test images to Planet's full daily archive would transform individual snapshots into a continuous "moving picture," enabling trend analyses and comparisons between fishing seasons. However, in the case of Planet Labs imagery, a refined methodology may need to be deployed in order to use images before 2018 due to changes in image resolution for tiles before this date.

In conclusion, this low-cost, open-source approach offers an accessible alternative to expensive satellite platforms. While single-moment counts cannot quantify fishing intensity outright or temporary migration patterns associated with the factories operations, they reveal pulses of activity that align with factory demand and local testimonies. As such, this method provides civil society groups, regulators, and researchers with a scalable tool for initial oversight, democratizing access to near-real-time information on artisanal fishing dynamics.

In its current form, the method does not reliably estimate vessel size beyond a basic distinction between small, medium, and merged shapes. At 3 m resolution, the typical six-meter pirogue hovers just at the edge of detectability, meaning fine-grained size estimation—critical for inferring catch volume—is highly uncertain. Side-by-side boats often appear as a single object, further complicating disaggregation. While larger vessels may appear more prominently and could be flagged manually, automating size-based classification at this resolution remains challenging. Future work could explore combining Planet imagery with higher-resolution datasets (e.g. drone or commercial sub-meter satellites) or incorporating shape descriptors to approximate vessel length more accurately. This would further permit the identification of larger vessels likely of Senegalese origin and provide deeper insights into temporary migration patterns associated with FMFO production in The Gambia. Conversely, the calculation of catch volume also depends on less visible factors such as gear type, fishing effort, and storage capacity, which remain beyond the scope of satellite imagery alone.

Although vessel counts alone cannot accurately predict total catch capacity or migration patterns, combining boat presence with contextual information—such as vessel size estimates with a thresholder approach, basket counts at landings, or known fishing effort—could offer a more holistic picture of artisanal fishing dynamics.